JACS
JOURNAL OF THE AMERICAN CHEMICAL SOCIETY
Article
pubs.acs.org/JACS

Ferromagnetic Ordering in Superatomic Solids

Chul-Ho Lee,[†,‡,§] Lian Liu,[‡] Christopher Bejger,[†] Ari Turkiewicz,[†] Tatsuo Goko,[‡] Carlos J. Arguello,[‡] Benjamin A. Frandsen,[‡] Sky C. Cheung,[‡] Teresa Medina,[∥] Timothy J. S. Munsie,[∥] Robert D'Ortenzio,[∥] Graeme M. Luke,[∥] Tiglet Besara,[⊥] Roger A. Lalancette,[▽] Theo Siegrist,[⊥,#] Peter W. Stephens,[○] Andrew C. Crowther,[◆] Louis E. Brus,[†] Yutaka Matsuo,[¶] Eiichi Nakamura,[¶] Yasutomo J. Uemura,[‡] Philip Kim,[+] Colin Nuckolls,[†] Michael L. Steigerwald,[†] and Xavier Roy*[,†]

[†]Department of Chemistry, Columbia University, New York, New York 10027, United States
[‡]Department of Physics, Columbia University, New York, New York 10027, United States
[§]KU-KIST Graduate School of Converging Science and Technology, Korea University, Seoul 136-701, Korea
[∥]Department of Physics and Astronomy, McMaster University, Hamilton, Ontario L8S 4L8, Canada
[⊥]National High Magnetic Field Laboratory, Florida State University, Tallahassee, Florida 32310, United States
[#]Department of Chemical and Biomedical Engineering, FAMU-FSU College of Engineering, Tallahassee, Florida 32310, United States
[▽]Department of Chemistry, Rutgers State University, Newark, New Jersey 07102, United States
[○]Department of Physics and Astronomy, Stony Brook University, Stony Brook, New York 11794, United States
[◆]Department of Chemistry, Barnard College, New York, New York 10027, United States
[¶]Department of Chemistry, The University of Tokyo, Tokyo 112-0033, Japan
[+]Department of Physics, Harvard University, Cambridge, Massachusetts 02138, United States

Supporting Information

ABSTRACT: In order to realize significant benefits from the assembly of solid-state materials from molecular cluster superatomic building blocks, several criteria must be met. Reproducible syntheses must reliably produce macroscopic amounts of pure material; the cluster-assembled solids must show properties that are more than simply averages of those of the constituent subunits; and rational changes to the chemical structures of the subunits must result in predictable changes in the collective properties of the solid. In this report we show that we can meet these requirements. Using a combination of magnetometry and muon spin relaxation measurements, we demonstrate that crystallographically defined superatomic solids assembled from molecular nickel telluride clusters and fullerenes undergo a ferromagnetic phase transition at low temperatures. Moreover, we show that when we modify the constituent superatoms, the cooperative magnetic properties change in predictable ways.

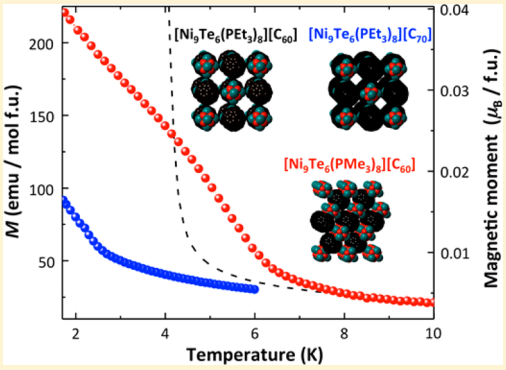

INTRODUCTION

Superatomic solids are three-dimensional periodic arrays in which the fundamental individual building blocks are independently prepared, electronically and structurally complementary molecular clusters.[1−3] Being completely tunable, these molecular cluster superatoms have discrete, well-defined structures and exhibit collective properties that are characteristic of and distributed over the entire cluster. The interaction of the individual cluster magnetic moments within the solids can create a long-range cooperative magnetically ordered phase that is distinct from the independent subunits: the binary compounds $[Ni_9Te_6(PEt_3)_8][C_{60}]$, $[Ni_9Te_6(PMe_3)_8][C_{60}]$, and $[Ni_9Te_6(PEt_3)_8][C_{70}]$ all show spontaneous magnetic ordering. Here we verify the bulk origin of the magnetic ordering in these materials by magnetic susceptibility and muon spin relaxation measurements. Furthermore, we show that the onset of the ferromagnetic transition can be adjusted by varying the intercluster interactions resulting from different crystal packing and electronic coupling.

Conventional and superatomic solids both have properties that are consequences of the attributes of the individual building blocks. Collective properties such as ferromagnetism, ferroelectricity, and superconductivity emerge as the result of long-range exchange interactions between the constituents.[4−8] In atomic solids, close-contacting atoms can interact to

Received: September 25, 2014
Published: November 7, 2014

   dx.doi.org/10.1021/ja5098622 | J. Am. Chem. Soc. 2014, 136, 16926−16931

generate long-range cooperative properties. Similar coupling between nanoscale building blocks could also arise in hierarchical arrays, but the assembly of strongly interacting cluster superlattices is problematic because the ligands that passivate the surface of superatoms typically physically separate the inorganic cores from one another and decrease the intercore coupling.[9,10] Nonetheless, short-range coupling of surface plasmons and excitons was reported in nanocrystal superlattices,[11] and short-range magnetic dipole interactions between superparamagnetic nanoparticles were shown to increase the blocking temperature of the assemblies.[12] In our materials, the magnetic moments of the superatomic molecular clusters can interact to produce long-range magnetic ordering.

RESULTS AND DISCUSSION

We assembled the solid-state binary superatom $[Ni_9Te_6(PEt_3)_8][C_{60}]$[3] from the electron-donating cluster $Ni_9Te_6(PEt_3)_8$[13] and the electron acceptor C_{60} (Figure 1a).

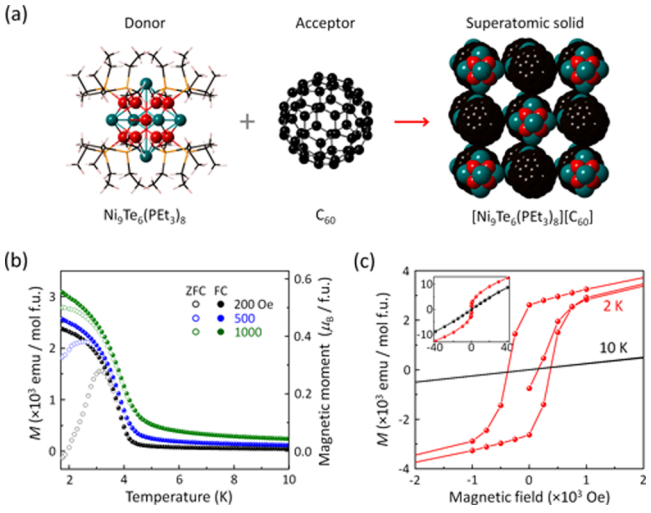

Figure 1. (a) Molecular structures of the superatomic building blocks $Ni_9Te_6(PEt_3)_8$ and C_{60} whose assembly creates the solid-state binary compound $[Ni_9Te_6(PEt_3)_8][C_{60}]$. Carbon, black; hydrogen, pink; nickel, red; phosphorus, orange; tellurium, teal. The phosphines have been removed to clarify the space-filling view of $[Ni_9Te_6(PEt_3)_8][C_{60}]$. (b) Temperature dependence of the ZFC and FC magnetizations of $[Ni_9Te_6(PEt_3)_8][C_{60}]$ in external applied magnetic fields of 200, 500, and 1000 Oe. (c) Magnetization of $[Ni_9Te_6(PEt_3)_8][C_{60}]$ as a function of the applied field above (10 K) and below (2 K) the transition temperature. The inset shows the high-field magnetization.

In-situ electron transfer between the electrically neutral superatoms in solution generates solid combinations of the clusters, and the inter-superatom electrostatic attraction creates the ionic binary superlattice. Rietveld refinement of the synchrotron powder X-ray diffraction (SPXRD) data indicates that the solid has a face-centered cubic structure analogous to the rock-salt crystal with a lattice parameter of 21.7 Å (see Figure S1 in the Supporting Information). We used Raman spectroscopy to examine the transfer of charge to the C_{60} in the binary superatom solids. The pentagonal A_{2g} pinch mode of C_{60}, centered at 1469 cm^{-1} for the electrically neutral species, monotonically shifts to lower energy with increasing negative charge.[14] The A_{2g} mode of C_{60} in the solid-state Raman spectrum of $[Ni_9Te_6(PEt_3)_8][C_{60}]$ is centered at 1453 cm^{-1}, indicating multiple electron transfers from the $Ni_9Te_6(PEt_3)_8$ cluster to C_{60} (Figure S4).

The magnetic behavior of the individual constituents has been reported. The molecular cluster $Ni_9Te_6(PEt_3)_8$ and the corresponding salts $[Ni_9Te_6(PEt_3)_8^{+}][BF_4^{-}]$ and $[Ni_9Te_6(PEt_3)_8^{2+}][BF_4^{-}]_2$ all have sizable magnetic moments at high temperature that become quenched upon cooling. In these cases, the clusters behave like isolated superparamagnets[15] that do not interact magnetically.[16,17] Fullerenes are diamagnetic compounds, and a few fulleride-containing salts exhibit long-range magnetic ordering of spins residing on the carbon clusters[18,19] or intercalated within the lattice.[20−24]

We made a preliminary report of superconducting quantum interference device (SQUID) magnetic susceptibility measurements on our superatom solids.[3] Above 10 K $[Ni_9Te_6(PEt_3)_8][C_{60}]$ exhibits Curie−Weiss behavior, following the relationship $\chi_M(T) = [C/(T - \Theta)] + \chi_D + \chi_{TIC}$, where C is the Curie constant, Θ is the Weiss constant, and χ_D and χ_{TIC} are the diamagnetic and temperature-independent contributions, respectively (Figure S5). We obtained a good fit to the data with C = 3.8 emu K Oe^{-1} (mol f.u.)$^{-1}$ (f.u. = formula unit), Θ = −7.4 K, χ_D = 0.002 emu Oe^{-1} (mol f.u.)$^{-1}$ and χ_{TIC} = 0.008 emu Oe^{-1} (mol f.u.)$^{-1}$. The small negative Weiss constant indicates weak antiferromagnetic interactions and suggests that each cluster subunit behaves as an isolated magnetic moment. Our analysis establishes a temperature-independent effective magnetic moment (μ_{eff}) of 5.4 μ_B/f.u. at an applied field of 1 T, but the location of the magnetic moments within the formula unit is still uncertain. Our Raman spectroscopy and magnetic susceptibility measurements confirm that the superatomic solid is qualitatively much different from a simple ionic solid such as $[Ni_9Te_6(PEt_3)_8^{2+}][BF_4^{-}]_2$.[16,17]

We sought to elaborate this difference by examining the magnetic behavior of $[Ni_9Te_6(PEt_3)_8][C_{60}]$ at lower temperatures. We found that the magnetic moments, which are independent at higher temperature, spontaneously couple to form a ferromagnetically ordered phase. Figure 1b shows the temperature dependence of the zero-field-cooled (ZFC) and field-cooled (FC) magnetizations for $[Ni_9Te_6(PEt_3)_8][C_{60}]$ at three different magnetic fields. In each case, we observed an abrupt change in magnetization at ∼4 K. In the ZFC measurements, we cooled the sample to 1.8 K in the absence of an applied magnetic field, then applied the indicated magnetic field once the sample had equilibrated at this low temperature, and finally observed the magnetization of the sample as we raised the temperature. In the FC measurements, we applied the indicated field at a temperature well above 4 K and then observed the magnetization as we reduced the temperature.[25] This abrupt transition at 4 K indicates the onset of spontaneous ferromagnetic ordering. As the strength of the magnetic field increases, the transition softens because the magnitude of the background signal increases. The magnetization of $[Ni_9Te_6(PEt_3)_8][C_{60}]$ reaches 3090 emu (mol f.u.)$^{-1}$ at 1.8 K with an applied external field of 1000 Oe, corresponding to a net magnetic moment of 0.55 μ_B/f.u.

The magnetic response of $[Ni_9Te_6(PEt_3)_8][C_{60}]$ to an external field changes dramatically upon cooling below the transition temperature. Figure 1c shows the field-dependent magnetization curves at two different temperatures. At 10 K the magnetization scales linearly with the applied magnetic field; however, at 2 K the magnetization curve is sigmoidal with a small coercive field of ∼400 Oe. This is consistent with long-range ferromagnetic ordering at that temperature. The hysteresis observed in this compound is noteworthy because C_{60} typically produces soft ferromagnets with no hysteresis.[26]

dx.doi.org/10.1021/ja5098622 | J. Am. Chem. Soc. 2014, 136, 16926−16931

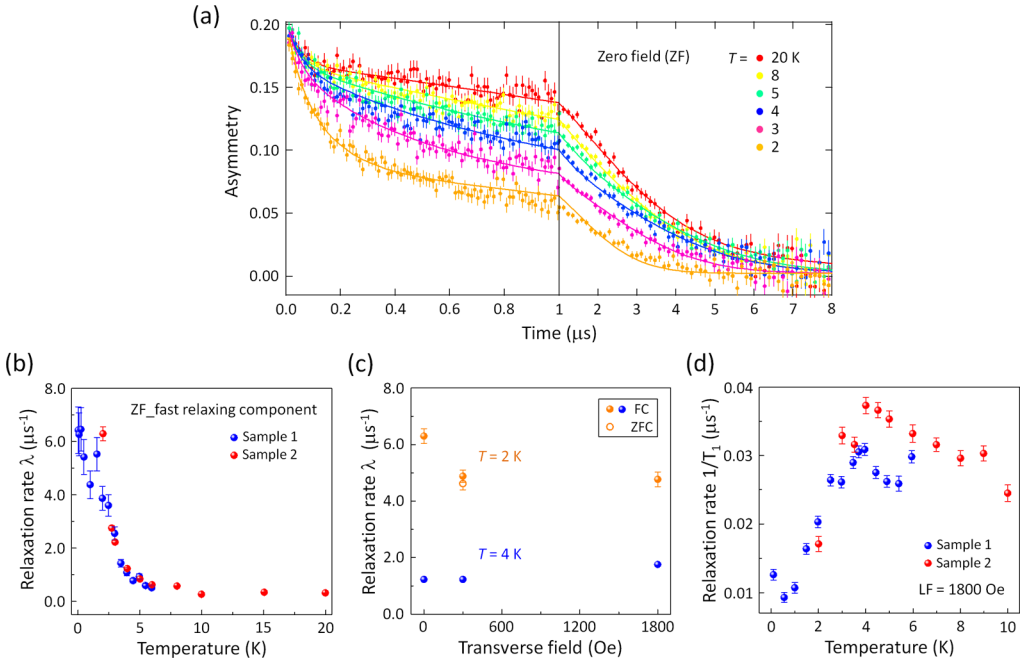

Figure 2. (a) Time spectra of muon spin relaxation measurements for $[Ni_9Te_6(PEt_3)_8][C_{60}]$. (b) Muon spin relaxation rate λ in zero field. Depicted is the exponential relaxation rate of the fast-relaxing component, representing about half of the muons implanted in the specimen. A sharp increase in λ below ~4 K reveals the onset of the static magnetic order. (c) Temperature dependence of the muon spin relaxation rate λ under a transverse external magnetic field. No difference between the results obtained in FC (solid symbols) and ZFC (open symbols) procedures was found. (d) Temperature dependence of the spin–lattice relaxation rate $1/T_1$ of positive muons with an applied longitudinal field (LF) of 1800 Oe. The sharp decrease in $1/T_1$ below ~4 K is due to static magnetic ordering.

Muon spin relaxation (MuSR) is a powerful probe[27,28] for detecting static magnetic order with ordered moments as small as 0.01 μ_B/f.u. in ferromagnetic (Ni, Fe, and MnSi[29]), antiferromagnetic,[30] and spin glass[31] systems. We therefore performed MuSR measurements to further understand the magnetic ordering in $[Ni_9Te_6(PEt_3)_8][C_{60}]$. In these experiments, we implanted spin-polarized positive muons in a polycrystalline sample and detected the positrons produced by the subsequent decay of the muons. The direction in which the decay positrons are emitted is specific to the muon spin direction and is locally affected by any magnetic ordering in the sample. While it does not provide direct information on spatial spin correlations, MuSR gives a measure of the volume fraction of the magnetically ordered region.[29,32] Whereas magnetization measurements reflect volume-integrated information, the volume-differential information provided by MuSR distinguishes bulk magnetic order from spurious effects of minority phases or impurities. This technique has been used to detect magnetic order and spin fluctuations in TDAE-C_{60},[18] (NH_3)-$K_{3-x}Rb_xC_{60}$,[33] and RbC_{60}[34] as well as superconductivity in alkali-metal-doped fullerenes A_3C_{60}.[35,36]

Our MuSR measurements confirm that the ferromagnetic ordering is characteristic of a large fraction of the sample volume. We performed MuSR measurements in zero-field (ZF), transverse field (TF), and longitudinal field (LF) geometries. Figure 2a shows the ZF MuSR time spectra of $[Ni_9Te_6(PEt_3)_8][C_{60}]$. We determined that the muons exhibit two relaxation rates (λ) when implanted in our sample: about half of the muons show fast relaxation at low temperatures with a relaxation rate of 6.52 μs^{-1}, while the rest of the muons undergo slow relaxation at a rate of 0.33 μs^{-1}. In an idealized sample with a magnetically ordered volume fraction of unity, the proportion of rapidly relaxing muons is 2/3 (see section VI in the Supporting Information for a detailed analysis of the MuSR data). Our results indicate that more than 80% of the entire volume undergoes static magnetic ordering. Our MuSR data cannot distinguish whether the remaining slowly relaxing signal is due to muons stopped in paramagnetic and/or nonmagnetic volumes or the result of muons that landed in a different crystallographic site where the local field from ordered moments nearly cancels out by symmetry.

Figure 2b shows the muon spin relaxation rate of the rapidly relaxing signal component of $[Ni_9Te_6(PEt_3)_8][C_{60}]$ as a function of temperature. Our analysis indicates that static magnetic ordering takes place at ~4 K. In addition, we estimated the ordered moment size from the relaxation rate in zero field and in transverse fields of 300 and 1800 Oe. Figure 2c shows that those values are nearly independent of the applied field, which is consistent with our magnetization results. The muon spin relaxation rate $(1/T_1)$ measured in a longitudinal field of 1800 Oe (Figure 2d) has a maximum at $T \approx 4$ K and is a further confirmation of magnetic order associated with critical behavior in dynamic spin fluctuations.[27]

The absence of long-lived muon spin precession in ZF has been observed in spin glasses[31] and in ferromagnetic systems such as $(Sr,Ca)RuO_3$.[29] This absence was ascribed to multiple muon sites and/or random fields associated with domain boundaries and demagnetization fields. In this context, the present MuSR results do not allow us to distinguish between two possible sources of magnetization hysteresis: ferromagnetic domain walls and spin-glass behavior. In one experiment (Figure 2c), we compared the muon spin relaxation rates measured in a transverse field of 300 Oe after the sample was cooled to 2 K in zero field (ZFC) and in a transverse field of 300 Oe (FC). We observed no measurable difference between the two protocols, indicating that the history dependence of the

dx.doi.org/10.1021/ja5098622 | J. Am. Chem. Soc. 2014, 136, 16926–16931

magnetic susceptibility is a result of the motion of macroscopic domains (for either the ferromagnetic or spin-glass case) and not of local spin reorientation. Conjointly, our SQUID magnetic susceptibility and MuSR data establish the *bulk* origin of the magnetic order in $[Ni_9Te_6(PEt_3)_8][C_{60}]$.

We performed independent SPXRD, SQUID magnetometry, and MuSR measurements on different samples that contained varying fractions of non-ferromagnetic amorphous material. Our measurements gave reproducible and mutually consistent results across all of the samples.

We can manipulate the structure of our superatom solid by modifying the molecular cluster building blocks, and in doing so we can change the magnetic behavior of the solids in predictable ways. We prepared and characterized three closely related materials: $[Ni_9Te_6(PMe_3)_8][C_{60}]$, $[Ni_9Te_6(PEt_3)_8][C_{70}]$, and $[Ni_9Te_6(PEt_3)_8][C_{61}H_2]$. Figure 3 shows the

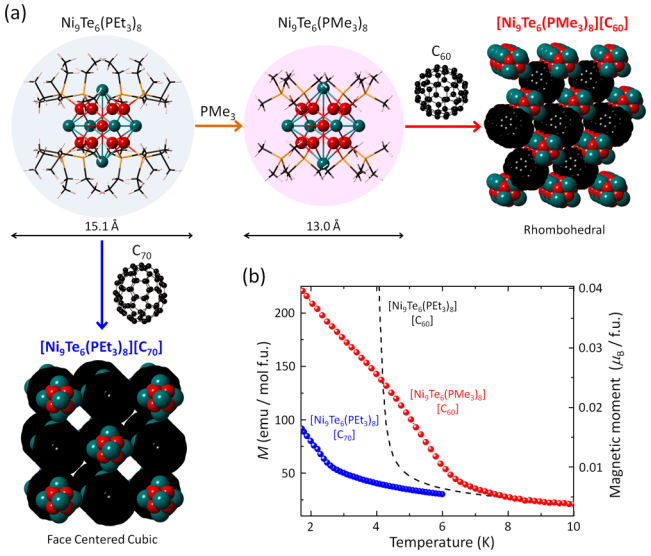

Figure 3. (a) Syntheses and crystal structures of $[Ni_9Te_6(PMe_3)_8][C_{60}]$ and $[Ni_9Te_6(PEt_3)_8][C_{70}]$. The molecular cluster $Ni_9Te_6(PMe_3)_8$ was prepared from $Ni_9Te_6(PEt_3)_8$ via ligand substitution. Carbon, black; hydrogen, pink; nickel, red; phosphorus, orange; tellurium, teal. The phosphines have been removed to clarify the space-filling views of $[Ni_9Te_6(PMe_3)_8][C_{60}]$ and $[Ni_9Te_6(PEt_3)_8][C_{70}]$. (b) Temperature dependence of the FC magnetizations of $[Ni_9Te_6(PEt_3)_8][C_{60}]$, $[Ni_9Te_6(PMe_3)_8][C_{60}]$, and $[Ni_9Te_6(PEt_3)_8][C_{70}]$ in an applied field of 100 Oe.

structures of the first two materials along with their FC magnetizations as functions of temperature. The compounds $[Ni_9Te_6(PEt_3)_8][C_{60}]$, $[Ni_9Te_6(PMe_3)_8][C_{60}]$, and $[Ni_9Te_6(PEt_3)_8][C_{70}]$ show qualitatively similar magnetic behaviors,[37] but there is a clear variation in the temperature of the ferromagnetic ordering.

The key difference between $[Ni_9Te_6(PEt_3)_8][C_{60}]$ and $[Ni_9Te_6(PMe_3)_8][C_{60}]$ is the relative size of the passivating ligand shell on the nickel telluride cluster. The use of trimethylphosphines in $[Ni_9Te_6(PMe_3)_8][C_{60}]$ leads to smaller superatom-to-superatom distances and a rhombohedral distortion of the rock-salt lattice. Reducing the size of the Ni_9Te_6 cluster enhances the electronic coupling between the core of the inorganic cluster and C_{60}. The distance between the donor and acceptor (as gauged by the distance between the centroid of the nickel telluride cluster and the centroid of the fullerene in the crystal structure) is reduced from 10.83 Å in $[Ni_9Te_6(PEt_3)_8][C_{60}]$ to 10.04 Å in $[Ni_9Te_6(PMe_3)_8][C_{60}]$. The Raman A_{2g} mode of $[Ni_9Te_6(PMe_3)_8][C_{60}]$ (1450 cm^{-1}) is shifted to lower energy compared with that of $[Ni_9Te_6(PEt_3)_8][C_{60}]$ (1453 cm^{-1}) (Figure S4), suggesting that in $[Ni_9Te_6(PMe_3)_8][C_{60}]$ the $Ni_9Te_6(PMe_3)_8$ cluster transfers more negative charge to the closer neighboring fullerene. The stronger electronic coupling in $[Ni_9Te_6(PMe_3)_8][C_{60}]$ moves the magnetic transition to a higher temperature of ~7 K.

Replacement of C_{60} with C_{70} in $[Ni_9Te_6(PEt_3)_8][C_{70}]$ retains the rock-salt structure with a slightly larger lattice parameter of 21.9 Å and lowers the magnetic transition temperature to ~2.5 K. The ellipsoidal C_{70} superatom must be disordered in the cubic structure, and this disorder is clearly visible in the SPXRD data (Figure S3). Raman spectroscopy confirms the transfer of charge from the nickel telluride cluster to C_{70} but does not allow us to make a direct comparison between $[Ni_9Te_6(PEt_3)_8][C_{70}]$ and the C_{60} compounds.

Single-crystal X-ray diffraction (SCXRD) determined that the solid $[Ni_9Te_6(PEt_3)_8][C_{61}H_2]$ assembles in a face-centered cubic structure analogous to that of $[Ni_9Te_6(PEt_3)_8][C_{60}]$. We collected the SCXRD data for the $C_{61}H_2$ compound at 100 K, and those data indicate a smaller unit cell (lattice parameter = 21.3 Å) than in the unit cell measured at room temperature for $[Ni_9Te_6(PEt_3)_8][C_{60}]$ (lattice parameter = 21.7 Å). In contrast to the superatomic solid-state compounds described above, $[Ni_9Te_6(PEt_3)_8][C_{61}H_2]$ does not exhibit magnetic ordering in the temperature range 1.8–293 K. We presume that the different magnetic behavior of $[Ni_9Te_6(PEt_3)_8][C_{61}H_2]$ is caused by the increase in energy and the loss of degeneracy of the $C_{61}H_2$ LUMO level[38] as well as the observed orientational disorder of the methylene group in the crystal.

CONCLUSION

We have demonstrated that long-range cooperative magnetic behaviors can emerge in superatomic solids assembled from superparamagnetic nickel telluride molecular clusters and fullerenes. These crystallographically defined ionic solids form by in situ electron transfer between electrically neutral building blocks. Magnetization and MuSR measurements confirmed the bulk origin of the magnetic order. Varying the physical size and shape of the superatomic ions can tune the magnetic properties of these materials. These results provide an unprecedented opportunity to design and create materials with multiple tunable functionalities and emergent cooperative properties.

EXPERIMENTAL SECTION

General Information. Triethylphosphine, trimethylphosphine, tellurium powder, and bis(cyclooctadiene)nickel(0) were obtained from Strem Chemicals. C_{60} and C_{70} were purchased from BuckyUSA. Dry and deoxygenated solvents were prepared by elution through a dual-column solvent system (Glass Contour Solvent Systems). All reactions and sample preparations were carried out under nitrogen using standard Schlenk techniques or in an argon-filled glovebox. $Ni_9Te_6(PEt_3)_6$ was synthesized according to a published protocol.[13]

Syntheses. *$[Ni_9Te_6(PEt_3)_8][C_{60}]$.* C_{60} (10 mg, 14 μmol) was dissolved in 2 mL of 1-methylnaphthalene, and the solution was filtered through a 0.2 μm syringe filter into a vial. 1-Methylnaphthalene (1 mL) and toluene (1 mL) were successively layered on top of the C_{60} solution. $Ni_9Te_6(PEt_3)_8$[13] (37 mg, 17 μmol) was dissolved in 5 mL of toluene, and this solution was filtered through a 0.2 μm syringe filter and layered on top of the C_{60} solution. The vial was placed in a freezer at −30 °C for 2 weeks. The supernatant solution was decanted, and the remaining black solid was centrifuged, rinsed with toluene, and

dx.doi.org/10.1021/ja5098622 | J. Am. Chem. Soc. 2014, 136, 16926–16931

dried in vacuo for ~12 h. Yield: 35 mg, 88% based on the amount of C_{60} used in the reaction. CCDC deposition number: 940472.

$Ni_9Te_6(PMe_3)_8$. $Ni_9Te_6(PEt_3)_8$ (70 mg, 31 μmol) was dissolved in 15 mL of toluene. An excess of trimethylphosphine (238 mg, 3.1 mmol) in toluene was added to the stirred $Ni_9Te_6(PEt_3)_8$ solution, and stirring was continued for ~12 h. The resulting suspension was left to stand at −40 °C, and the supernatant was decanted. The solid product was rinsed with hexanes and dried in vacuo for ~12 h. Samples suitable for SCXRD were obtained by crystallization from hot toluene (~65 °C). Yield: 41 mg, 69%. CCDC deposition number: 1021518.

$[Ni_9Te_6(PMe_3)_8][C_{60}]$. C_{60} (10 mg, 14 μmol) was dissolved in 5 mL of toluene, and the solution was filtered with a 0.2 μm syringe filter into a vial. $Ni_9Te_6(PMe_3)_8$ (36 mg, 19 μmol) was partially dissolved in 5 mL of toluene, and the mixture was filtered (the cluster solubility was noticeably poor). The resulting solution was added dropwise to the stirred C_{60} solution. The slurry was then stirred for 5 min. The solid was centrifuged, rinsed with toluene, and dried in vacuo for ~12 h. Yield: 7 mg, 20% based on the amount of C_{60} used in the reaction. CCDC deposition number: 1003886.

$[Ni_9Te_6(PEt_3)_8][C_{70}]$. Prepared analogously to $[Ni_9Te_6(PEt_3)_8][C_{60}]$ using C_{70} (10 mg, 12 μmol) and $Ni_9Te_6(PEt_3)_8$ (32 mg, 14 μmol). Yield: 35 mg, 94% based on the amount of C_{70} used in the reaction. CCDC deposition number: 1003708.

$[Ni_9Te_6(PEt_3)_8][C_{61}H_2]$. Prepared analogously to $[Ni_9Te_6(PEt_3)_8][C_{60}]$ using $C_{61}H_2$[38] (10 mg, 14 μmol) and $Ni_9Te_6(PEt_3)_8$ (40 mg, 18 μmol). Yield: 10 mg, 25% based on the amount of $C_{61}H_2$ used in the reaction.

Magnetometry. The magnetic data were collected on a Quantum Design SQUID magnetometer. The samples were encapsulated in a gel capsule under an atmosphere of Ar.

MuSR. The data were obtained at TRIUMF (Vancouver, BC) by implanting positive muons in polycrystalline specimens and detecting their decay positrons emitted preferentially to the muon spin directions.

X-ray Diffraction. High-resolution SPXRD measurements were performed at ambient temperature (~295 K) on the X16C beamline at the National Synchrotron Light Source at Brookhaven National Laboratory. A Si(111) channel-cut monochromator selected a parallel incident beam. The diffracted X-rays were analyzed using a Ge(111) crystal and detected using a NaI scintillation counter. The powder was sealed in a glass capillary of 1 mm nominal diameter, which was spun at several hertz during data collection to improve the particle statistics. Data were collected over the 2θ range from 1° to 30° in steps of 0.005°, with the count time increasing from 10 to 30 s per point over that range.

Raman Spectroscopy. Raman measurements were performed on a home-built confocal micro-Raman spectrometer. The samples were air-sensitive, so all of the measurements were performed in cuvettes sealed under an atmosphere of Ar. A 40×/0.6 NA objective lens focused a 633 nm helium−neon laser onto the sample with a 1 μm^2 spot size. The scattered light passed through a 633 nm long-pass filter and was dispersed by a 0.27 m monochromator onto an array detector. The laser power at the sample ranged from 15 to 40 μW, giving power densities ranging from 1.5 to 4 kW/cm^2. The power densities were kept low to prevent sample degradation. Averaging was performed for 900 to 1800 s.

■ ASSOCIATED CONTENT

Supporting Information

Synthetic and measurement details, X-ray diffraction, Raman spectroscopy, magnetometry, analysis of MuSR data, and a zip file containing crystallographic files (CIF). This material is available free of charge via the Internet at http://pubs.acs.org.

■ AUTHOR INFORMATION

Corresponding Author

xr2114@columbia.edu

Notes

The authors declare no competing financial interest.

■ ACKNOWLEDGMENTS

This material is based upon work supported by the Air Force Office of Scientific Research under AFOSR Award FA9550-14-1-0381. MuSR experiments were supported by the U.S. NSF Partnership for International Research and Education (PIRE) (OISE-0968226) and DMR-1105961 Projects at Columbia; the JAEA Reimei Project at Columbia; and NSERC and CIFAR at McMaster. This work was supported in part by the FAME Center, one of six centers of STARnet, a Semiconductor Research Corporation program sponsored by MARCO and DARPA. The National Synchrotron Light Source at Brookhaven National Laboratory was supported by the U.S. Department of Energy, Office of Basic Energy Sciences, under Contract DE-AC02-98CH10886. A.T. thanks the Société de Chimie Industrielle Scholarship Program and the Columbia University Egleston Scholars Program. T.B. and T.S. were supported by the U.S. Department of Energy, Office of Basic Energy Sciences, under Contract DE-SC0008832, and a portion of this work was performed at the National High Magnetic Field Laboratory, which is supported by the National Science Foundation (Cooperative Agreement DMR-1157490), the State of Florida, and the U.S. Department of Energy. This work was supported by MEXT, Japan (KAKENHI Specially Promoted Research; grant # 22000008 to E.N.). C.B. thanks the Camille and Henry Dreyfus Postdoctoral Program in Environmental Chemistry.

■ REFERENCES

(1) Claridge, S. A.; Castleman, A. W., Jr.; Khanna, S. N.; Murray, C. B.; Sen, A.; Weiss, P. S. *ACS Nano* **2009**, *3*, 244.
(2) Khanna, S. N.; Jena, P. *Phys. Rev. B* **1995**, *51*, 13705.
(3) Roy, X.; Lee, C.-H.; Crowther, A. C.; Schenck, C. L.; Besara, T.; Lalancette, R. A.; Siegrist, T.; Stephens, P. W.; Brus, L. E.; Kim, P.; Steigerwald, M. L.; Nuckolls, C. *Science* **2013**, *341*, 157.
(4) Miller, J. S.; Epstein, A. J.; Reiff, W. M. *Chem. Rev.* **1988**, *88*, 201.
(5) Reveles, J. U.; Clayborne, P. A.; Reber, A. C.; Khanna, S. N.; Pradhan, K.; Sen, P.; Pederson, M. R. *Nat. Chem.* **2009**, *1*, 310.
(6) Zhang, X. X.; Wang, Y.; Wang, H. P.; Lim, A.; Gantefoer, G.; Bowen, K. H.; Reveles, J. U.; Khanna, S. N. *J. Am. Chem. Soc.* **2013**, *135*, 4856.
(7) Jerome, D.; Mazaud, A.; Ribault, M.; Bechgaard, K. *J. Phys., Lett.* **1980**, *41*, L95.
(8) Aoyagi, S.; Nishibori, E.; Sawa, H.; Sugimoto, K.; Takata, M.; Miyata, Y.; Kitaura, R.; Shinohara, H.; Okada, H.; Sakai, T.; Ono, Y.; Kawachi, K.; Yokoo, K.; Ono, S.; Omote, K.; Kasama, Y.; Ishikawa, S.; Komuro, T.; Tobita, H. *Nat. Chem.* **2010**, *2*, 678.
(9) Murray, C. B.; Kagan, C. R.; Bawendi, M. G. *Annu. Rev. Mater. Sci.* **2000**, *30*, 545.
(10) Kovalenko, M. V.; Scheele, M.; Talapin, D. V. *Science* **2009**, *324*, 1417.
(11) Shimizu, K. T.; Woo, W. K.; Fisher, B. R.; Eisler, H. J.; Bawendi, M. G. *Phys. Rev. Lett.* **2002**, *89*, No. 117401.
(12) Laurent, S.; Forge, D.; Port, M.; Roch, A.; Robic, C.; Elst, L. V.; Muller, R. N. *Chem. Rev.* **2008**, *108*, 2064.
(13) Brennan, J. G.; Siegrist, T.; Stuczynski, S. M.; Steigerwald, M. L. *J. Am. Chem. Soc.* **1989**, *111*, 9240.
(14) Kuzmany, H.; Matus, M.; Burger, B.; Winter, J. *Adv. Mater.* **1994**, *6*, 731.
(15) The difference between paramagnetic and superparamagnetic behaviors is somewhat ambiguous in molecular clusters. The effective magnetic moment of the nickel telluride cluster is smaller than the moment expected assuming spin-only atomic contributions, suggesting that the atomic moments are exchange-coupled and behave as a single

unit. For an in-depth discussion, see: Khanna, S. N.; Linderoth, S. *Phys. Rev. Lett.* **1991**, *67*, 742. Also see refs 16 and 17 for a full description of the magnetic behavior of the clusters $[Ni_9Te_6(PEt_3)]^{n+}$ with n = 0, 1, and 2.

(16) Palstra, T. T. M.; Steigerwald, M. L.; Ramirez, A. P.; Kwon, Y. U.; Stuczynski, S. M.; Schneemeyer, L. F.; Waszczak, J. V.; Zaanen, J. *Phys. Rev. Lett.* **1993**, *71*, 1768.

(17) Palstra, T. T. M.; Steigerwald, M. L.; Ramirez, A. P.; Zaanen, J. *Physica B* **1994**, *199*, 619.

(18) Lappas, A.; Prassides, K.; Vavekis, K.; Arcon, D.; Blinc, R.; Cevc, P.; Amato, A.; Feyerherm, R.; Gygax, F. N.; Schenck, A. *Science* **1995**, *267*, 1799.

(19) Mrzel, A.; Omerzu, A.; Umek, P.; Mihailovic, D.; Jaglicic, Z.; Trontelj, Z. *Chem. Phys. Lett.* **1998**, *298*, 329.

(20) Ishii, K.; Fujiwara, A.; Suematsu, H.; Kubozono, Y. *Phys. Rev. B* **2002**, *65*, No. 134431.

(21) Margiolaki, I.; Margadonna, S.; Prassides, K.; Hansen, T.; Ishii, K.; Suematsu, H. *J. Am. Chem. Soc.* **2002**, *124*, 11288.

(22) Maruyama, Y.; Motohashi, S.; Suzuki, K.; Takagi, S.; Ogata, H. *Solid State Commun.* **2000**, *115*, 457.

(23) Maruyama, Y.; Motohashi, S.; Sakai, N.; Watanabe, K.; Suzuki, K.; Ogata, H.; Kubozono, Y. *Solid State Commun.* **2002**, *123*, 229.

(24) Takenobu, T.; Chi, D. H.; Margadonna, S.; Prassides, K.; Kubozono, Y.; Fitch, A. N.; Kato, K.; Iwasa, Y. *J. Am. Chem. Soc.* **2003**, *125*, 1897.

(25) We observed some irreversibility between the ZFC and FC magnetizations of $[Ni_9Te_6(PEt_3)_8][C_{60}]$. This irreversibility may be attributed to the presence of large barriers to rotation of the sample magnetization due to state pinning in a disordered structure (see ref 39).

(26) Allemand, P. M.; Khemani, K. C.; Koch, A.; Wudl, F.; Holczer, K.; Donovan, S.; Gruner, G.; Thompson, J. D. *Science* **1991**, *253*, 301.

(27) Lee, S. L.; Kilcoyne, S. H.; Cywinski, R. *Muon Science: Muons in Physics, Chemistry and Materials*; Institute of Physics Publishing: Bristol, UK, 1999.

(28) Hayano, R. S.; Uemura, Y. J.; Imazato, J.; Nishida, N.; Yamazaki, T.; Kubo, R. *Phys. Rev. B* **1979**, *20*, 850.

(29) Uemura, Y. J.; Goko, T.; Gat-Malureanu, I. M.; Carlo, J. P.; Russo, P. L.; Savici, A. T.; Aczel, A.; MacDougall, G. J.; Rodriguez, J. A.; Luke, G. M.; Dunsiger, S. R.; McCollam, A.; Arai, J.; Pfleiderer, C.; Boni, P.; Yoshimura, K.; Baggio-Saitovitch, E.; Fontes, M. B.; Larrea, J.; Sushko, Y. V.; Sereni, J. *Nat. Phys.* **2007**, *3*, 29.

(30) Luetkens, H.; Klauss, H. H.; Kraken, M.; Litterst, F. J.; Dellmann, T.; Klingeler, R.; Hess, C.; Khasanov, R.; Amato, A.; Baines, C.; Kosmala, M.; Schumann, O. J.; Braden, M.; Hamann-Borrero, J.; Leps, N.; Kondrat, A.; Behr, G.; Werner, J.; Buchner, B. *Nat. Mater.* **2009**, *8*, 305.

(31) Uemura, Y. J.; Yamazaki, T.; Harshman, D. R.; Senba, M.; Ansaldo, E. J. *Phys. Rev. B* **1985**, *31*, 546.

(32) Uemura, Y. J.; Aczel, A. A.; Ajiro, Y.; Carlo, J. P.; Goko, T.; Goldfeld, D. A.; Kitada, A.; Luke, G. M.; MacDougall, G. J.; Mihailescu, I. G.; Rodriguez, J. A.; Russo, P. L.; Tsujimoto, Y.; Wiebe, C. R.; Williams, T. J.; Yamamoto, T.; Yoshimura, K.; Kageyama, H. *Phys. Rev. B* **2009**, *80*, No. 174408.

(33) Arvanitidis, J.; Papagelis, K.; Takabayashi, Y.; Takenobu, T.; Iwasa, Y.; Rosseinsky, M. J.; Prassides, K. *J. Phys.: Condens. Mater.* **2007**, *19*, No. 386235.

(34) Uemura, Y. J.; Kojima, K.; Luke, G. M.; Wu, W. D.; Oszlanyi, G.; Chauvet, O.; Forro, L. *Phys. Rev. B* **1995**, *52*, R6991.

(35) Uemura, Y. J.; Keren, A.; Le, L. P.; Luke, G. M.; Sternlieb, B. J.; Wu, W. D.; Brewer, J. H.; Whetten, R. L.; Huang, S. M.; Lin, S.; Kaner, R. B.; Diederich, F.; Donovan, S.; Gruner, G.; Holczer, K. *Nature* **1991**, *352*, 605.

(36) Kiefl, R. F.; Macfarlane, W. A.; Chow, K. H.; Dunsiger, S.; Duty, T. L.; Johnston, T. M. S.; Schneider, J. W.; Sonier, J.; Brard, L.; Strongin, R. M.; Fischer, J. E.; Smith, A. B. *Phys. Rev. Lett.* **1993**, *70*, 3987.

(37) The absolute magnitudes of the magnetizations are smaller and the transitions are softer in both $[Ni_9Te_6(PMe_3)_8][C_{60}]$ and $[Ni_9Te_6(PEt_3)_8][C_{70}]$ relative to $[Ni_9Te_6(PEt_3)_8][C_{60}]$. We are not yet certain of the source(s) of this, but in both cases the magnetometry samples contained significant volume fractions of amorphous material, and that of $[Ni_9Te_6(PMe_3)_8][C_{60}]$ also contained a small amount of a crystalline impurity that we have not been able to identify. We could not measure the magnetic hysteresis loop in these samples.

(38) Zhang, Y.; Matsuo, Y.; Li, C.-Z.; Tanaka, H.; Nakamura, E. *J. Am. Chem. Soc.* **2011**, *133*, 8086.

(39) Buschmann, W. E.; Paulson, S. C.; Wynn, C. M.; Girtu, M. A.; Epstein, A. J.; White, H. S.; Miller, J. S. *Adv. Mater.* **1997**, *9*, 645.